

Journal of Materials Chemistry C

Accepted Manuscript



This is an *Accepted Manuscript*, which has been through the Royal Society of Chemistry peer review process and has been accepted for publication.

Accepted Manuscripts are published online shortly after acceptance, before technical editing, formatting and proof reading. Using this free service, authors can make their results available to the community, in citable form, before we publish the edited article. We will replace this *Accepted Manuscript* with the edited and formatted *Advance Article* as soon as it is available.

You can find more information about *Accepted Manuscripts* in the [Information for Authors](#).

Please note that technical editing may introduce minor changes to the text and/or graphics, which may alter content. The journal's standard [Terms & Conditions](#) and the [Ethical guidelines](#) still apply. In no event shall the Royal Society of Chemistry be held responsible for any errors or omissions in this *Accepted Manuscript* or any consequences arising from the use of any information it contains.

Journal Name

Dynamic Article Links ►

Cite this: DOI: 10.1039/c0xx00000x

www.rsc.org/xxxxxx

ARTICLE TYPE

Reversible Thermal-Mode Control of Luminescence from Liquid-Crystalline Gold(I) Complexes

Kaori Fujisawa,^{a,b} Yuki Okuda,^a Yuichi Izumi,^a Akira Nagamatsu,^a Yuki Rokusha,^a Yusuke Sadaike,^a Osamu Tsutsumi^{a,b,*}

⁵ Received (in XXX, XXX) Xth XXXXXXXXXX 20XX, Accepted Xth XXXXXXXXXX 20XX

DOI: 10.1039/b000000x

The synthesis and characterisation of liquid-crystalline (LC) gold complexes designed to have a rod-like structure in dimeric form is described, and the relationship between their photophysical properties and aggregated structure is discussed. The luminescence intensities of the complexes were enhanced in the condensed phase, meaning that the complexes showed aggregation-induced emission. Observed photoluminescence in the condensed phase could be assigned to a monomer emission; however, luminescent properties were strongly affected by the aggregated structures of the complexes. A reversible “on-off” switching of the luminescence induced by the phase transition between LC and isotropic phases was demonstrated. Moreover, complex **1b** showed thermochromic photoluminescence controlled by the aggregated structure; the colour of luminescence could be reversibly controlled by the phase transition between crystalline and LC phases. These LC gold complexes show potential application as materials for novel light-emitting devices.

Introduction

Organic materials showing strong luminescence in the condensed phase have attracted great interest in view of their potential application toward light-emitting devices.¹ In general, however, the luminescence of such materials is strongly reduced in the condensed phase because of the concentration quenching effect; namely, luminescence is quenched by the aggregation of luminescent organic molecules, preventing them from being used in practical devices. Recently, materials showing aggregation-induced emission (AIE) have been developed,² whereby materials exhibiting AIE properties show enhanced luminescence via molecular aggregation—in contrast to quenching at high concentrations—in the condensed phase.

Gold complexes are known to exhibit photoluminescence with quantum yields (Φ) of 0.5–0.9 in cases of intermolecular interaction between gold atoms (aurophilic interaction);³ that is, luminescence generated by these complexes is enhanced by molecular aggregation in the condensed phases. For this reason, gold complexes have emerged as promising candidates for AIE

materials with potential applicability to practical devices.³ In addition, the properties of the luminescence derived from gold complexes are structure-dependent⁴ such that colour and/or luminescence intensity can be manipulated by control of aggregate structure.⁵ So far, several types of liquid-crystalline (LC) gold complexes have been developed with the aim of controlling their aggregate structure.⁶ Some useful characteristics of LCs that lend themselves to efficient aggregate control include their self-assembled nature, fluidity, and responsiveness to external stimuli.⁷ In this study, we examine the aggregation and photoluminescence behaviours of gold complexes in both crystalline and LC phases, providing a discussion of the relationship between the aggregated structure and luminescent properties. In particular, we report that a reversible change in the luminescent colour can be induced by precise control of aggregate structure.

Our strategy toward molecular design to provide a strong intermolecular interaction for facile formation of molecular aggregates was the introduction of simple and non-bulky ligands onto the gold atom to suppress the effects of steric hindrance. Thus, we synthesised Au(I) complexes having 4-alkoxyphenylisocyanide and chlorine atoms as ligands, as shown in Fig. 1 (**1a–c**; $n = 5–7$). Molecules showing calamitic LC phases are generally designed to have rod-like structures; for this reason, most calamitic LC molecules usually consist of a rigid multi-ring system, *e.g.*, biphenyl, phenyl benzoate, diphenylacetylene, azobenzene, *etc.* However, since we introduced simple phenyl isocyanide ligands to avoid steric hindrance, the molecular structures of gold complexes designed in this study are quite different from conventional calamitic mesogens. It has been reported that gold complexes tend to form dimers in the LC phase, with the dimer acting as one unit of the mesogen,⁸ accordingly, we designed the molecules so as to incorporate a two-ring system into the rod-like structure by dimer formation.

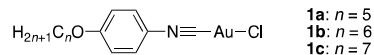


Fig. 1 Structure of Au complexes used in this study.

Results and discussion

Synthesis and characterisation of gold complexes

Complexes **1a–c** were synthesised by the method previously reported by Coco *et al.*⁹ The isocyanide ligands were first prepared (see ESI[†]), followed by synthesis of Au complex **1** by reaction with (tht)AuCl (tht = tetrahydrothiophene). The complexes were purified by recrystallisation from acetonitrile and were obtained as colourless crystals. The complexes were fully characterised by ¹H NMR, HRMS, IR, and elemental analysis. All analytical data are given in the Experimental section and indicate that the desired compounds were obtained.

Thermal stabilities of the complexes were evaluated by thermogravimetric analysis (TGA). It was confirmed by TGA that the compounds were thermally stable up to 248–262 °C, with the thermal decomposition temperature defined as the temperature at which 5% weight loss had occurred (Fig. S1). To clarify the actual molecular structures of complexes **1a–c** in the condensed phase, single-crystal X-ray structural analyses were performed. The crystal packing structures of the complexes are shown in Fig. 2, and selected interatomic distances between neighbouring molecules are listed in Table 1. The key crystallographic data are also summarised in Table S1. In the crystals of **1a–c**, the intermolecular Au•••Au distance was approximately 3.3 Å, substantially shorter than the sum of van der Waals radii (3.8 Å) of two gold atoms;¹⁰ this result is suggestive of the existence of an aurophilic interaction between neighbouring molecules. The stabilisation energy of the aurophilic interaction is as large as that of the hydrogen bond;^{10,11} we can therefore consider that this interaction provides further stability to the dimeric complex.

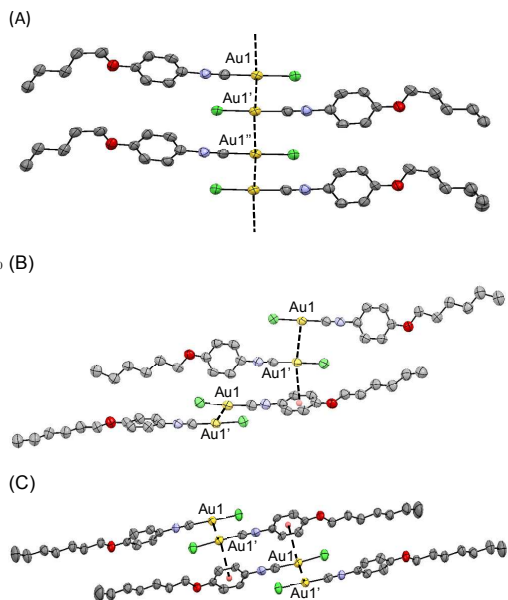


Fig. 2 Crystal structures of complexes **1a–c** at room temperature: (A) **1a**; (B) **1b**; (C) **1c**. Existence of intermolecular Au•••Au and Au•••π interactions are indicated with broken lines. For clarity, only the major components are shown and protons are omitted. Atom colour legend: grey, C; green, Cl; purple, N; red, O; yellow, Au; pink, centroid of phenyl ring.

Table 1 Selected distances (Å) and angles (°) between neighbouring molecules in crystals of **1a–c**.

	1a	1b	1c
Au1•••Au1'	3.342(1)	3.3810(5)	3.3092(6)
Au1'•••Au1''	3.342(1)	–	–
Au•••Ph ^a	3.516	3.592	3.538
θ^b	3.3	6.0	5.0

^a Distance between the Au atom and centroid of the phenyl ring in a neighbouring molecule. ^b Angle between the vector normal to the aromatic ring and that passing through the centroid to the Au atom.

As shown in Fig. 2, the aurophilic interaction of complex **1a** was extended; as a result, crystal **1a** formed a linear polymer structure without covalent bonds between each repeating unit. Furthermore, the Au atom appeared close to the phenyl ring of a neighbouring molecule that was involved in the formation of another polymer chain *via* Au•••Au interaction (Fig. S3); the distance between the Au atom and centroid of the phenyl ring was found to be 3.516 Å, and the angle between the vector normal to the aromatic ring and that passing through the centroid to the Au atom (θ) was 3.3°. Generally, Au(I) complexes form aggregates based on the interaction between Au atoms and an aromatic π -electron system when the distance between them is less than 4.0 Å, with angle θ equal to or less than 20°. From the geometric parameters obtained from single-crystal structural analysis of **1a**, we can also conclude the presence of an intermolecular Au••• π interaction, *i.e.* in addition to an aurophilic interaction, the polymer chains were additionally cross-linked through a Au••• π contact. A similar intermolecular Au••• π interaction was also found in complexes **1b** and **1c**. In contrast, the aurophilic contact was not extended in these two complexes; the interatomic distances between the second neighbouring Au atoms were longer than 3.8 Å and did not form linear polymer structures, instead existing as isolated tetramers in the crystals (Fig. 2). The melting point of **1a** (134 °C) was significantly higher than those of the others (**1b**: 121 °C; **1c**: 124 °C). The difference in melting points between **1a** and the other complexes can be explained by the presence of the cross-linked polymer structure formed through both aurophilic and Au••• π interactions.

Liquid crystalline behaviour

LC phase transition behaviours of **1a–c** were studied using polarised optical microscopy (POM), differential scanning calorimetry (DSC), and powder X-ray diffractometry (XRD). All complexes used in this study showed enantiotropic LC phases. POM observations at the LC temperature revealed a typical fan shape (Fig. 3), indicating that the complexes form a smectic (Sm) phase. Detailed LC phase structural analyses were determined by powder XRD (Fig. 4 for **1b** as a representative example, and Figs. S4 and S5). The phase sequences and phase transition temperatures (defined as the onset temperature of DSC peaks) of **1a–c** are summarised in Table 2. All complexes showed polymorphism in the crystalline phase. Especially, **1b** showed many unidentified complex crystalline phases in the cooling process.

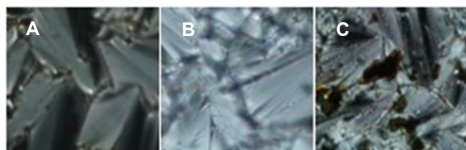


Fig. 3 Optical texture of complexes observed by POM: (A) **1a** at 157 °C; (B) **1b** at 155 °C; (C) **1c** at 147 °C. All photographs were taken during the first cooling scan.

Table 2 Phase transition behaviour of complexes **1a-c**.

	Phase sequences and transition temperature (°C) ^a	
1a	Heating	Cr ₁ 100 Cr ₂ 134 Sm 158 I
	Cooling	Cr ₁ 83 Cr ₂ 120 Sm 157 I
1b	Heating	Cr ₁ 59 Cr ₂ 79 Cr ₃ 121 SmC 166 I
	Cooling	Cr _x ^b 110 SmC 166 I
1c	Heating	Cr ₁ 87 Cr ₂ 124 SmC 172 I
	Cooling	Cr ₁ 72 Cr ₂ 121 SmC 172 I

^a Abbreviations: Cr, crystalline; Sm, smectic; I, isotropic. ^b Below 110 °C, many unidentified crystalline phases were observed (see Fig. S2b in ESI[†]).

The molecular structures of complexes **1a-c** appeared different from those of typical rod-like calamitic LC molecules; however, as mentioned above, complexes **1a-c** formed dimers with antiparallel orientations in the crystalline phase, with the dimers adopting a symmetric rod-like structure. In analogy to other LC gold complexes reported previously,⁸ we can consider that complexes **1a-c** form the dimer in the Sm phase, and that the dimer acts as a unit mesogen. The results of XRD analysis support the hypothesis that the complexes formed dimers in the LC phase; the interlayer spacing of the Sm phase of **1b** was estimated as 27 Å by XRD, as shown in Fig. 4, which is noticeably larger than the molecular length of the monomer of **1b** (17.9 Å), but slightly smaller than the length of the dimer (32.2 Å) formed by the auriphilic interaction. Therefore, it is reasonable to assume that the Au complex dimer acts as the unit mesogen, and we can conclude that the tilted mesogens (dimers) are packed into the Sm layer to form a smectic C (SmC) phase with a tilt angle (defined as the angle between the vector normal to the Sm layer and long axis of the mesogen) of 33°, as schematically illustrated in Fig. 5. A further discussion of obtained XRD data as it relates to phase identity and luminescence properties of **1b** is provided later in this report.

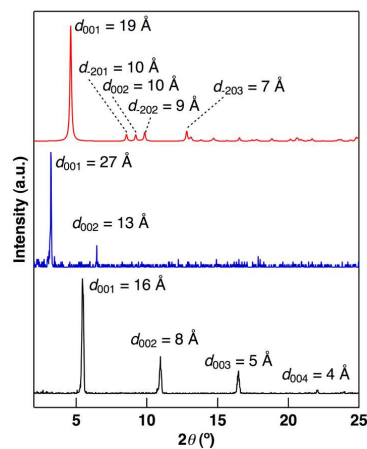


Fig. 4 XRD patterns of **1b**: Cr₁ phase at 25 °C simulated from single crystal X-ray structural analysis (red); SmC phase at 130 °C (blue); Cr_x phase at 40 °C obtained by recrystallisation of SmC phase after cooling (black).

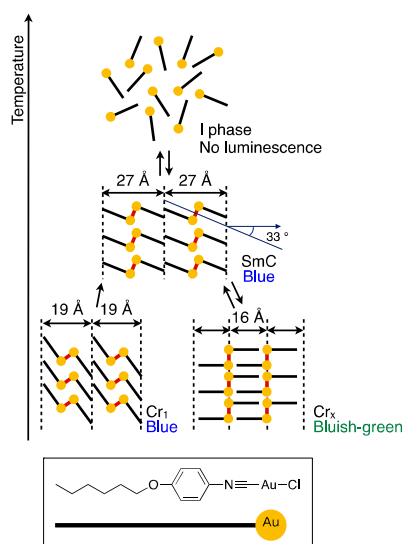


Fig. 5 Schematic illustration of unit mesogen structural model and plausible molecular packing structure in crystalline and LC phases of complex **1b**.

Photophysical properties of the complexes

Photophysical properties of the gold complexes were observed both in crystalline and dilute solutions; Fig. 6A shows the absorption, photoluminescence, and excitation spectra of complex **1b**. An absorption band appeared at ~280 nm in solution (CH₂Cl₂, 1 × 10⁻⁴ mol L⁻¹; dielectric constant = 8.93). In another solvent,

e.g. in CHCl_3 (dielectric constant = 4.81), the complex showed similarly shaped bands at the same wavelength in the absorption spectrum, meaning that a shift in the absorption spectrum was not induced by solvent polarity. In addition, the complex exhibited strong photoluminescence in the crystalline phase. However, the complex showed no photoluminescence in dilute solution ($1 \times 10^{-6} \text{ mol L}^{-1}$), while only very weak photoluminescence with the same spectral shape as in crystal was observed in a more concentrated solution ($1 \times 10^{-4} \text{ mol L}^{-1}$, Fig. 6B).

The above results clearly indicate that photoluminescence was emitted from the complex aggregates, but that the complex did not emit luminescence in the monomeric form. The excitation spectrum of the crystalline phase did not show overlap with the absorption spectrum of the dilute solution (Fig. 6A), an observation that also supports our hypothesis that the luminescence was in fact aggregate-induced. An emission band appeared at around 450 nm with vibronic structures both in the crystalline phase (Fig. 6A) and in solution (Fig. 6B). It has been reported that photoluminescence resulting from an aurophilic interaction can be generally observed as a broad luminescence band in the longer wavelength region.^{3,13} The emission band at ~450 nm with vibronic structure has been suggested to be either a ligand-to-metal charge transfer (LMCT) or ligand-based $\pi-\pi^*$ transition.¹³ In the present complexes, the electronic transition for photoluminescence at 450 nm is currently unclear, but we should consider that this luminescence is emitted from an excited state localised in a single molecule—namely, monomer emission. However, since no luminescence was observed under dilute conditions, i.e., when the species were isolated as the single molecule in dilute solution, we can thus conclude that this photoluminescence was the result of AIE. Internal molecular motion, which results in non-radiative deactivation of the excited state, may be hindered by aggregation. As a result, the complex showed AIE. The same photophysical properties were observed for the other complexes in both the crystalline phase and in solution.

The photoluminescence lifetimes (τ) of **1a–c** were also measured in the crystalline phase (Table 3 and Fig S10). The complexes showed single exponential decay photoluminescence profiles, except for complex **1c**, where a bi-exponential decay profile was observed. The τ for all the complexes were on the microsecond timescale, meaning that the observed photoluminescence was phosphorescence. The bi-exponential decay indicates the existence of two kinds of luminescent sites in the crystals of complex **1c**. By comparison with complexes **1a** and **1b**, we speculate that the luminescent site with longer lifetime, which is the minor component of the decay, is the same as that in the other complexes. The crystal structure of **1c** is quite different from the others; **1c** was crystallised in the triclinic space group $P\bar{1}$, but the others were crystallised in the monoclinic space group $P2_1/a$ (Table S1). Therefore, we consider that luminescence with the shorter lifetime, which is the major component, was emitted from crystals with the triclinic space group $P\bar{1}$, and that the crystal with the monoclinic space group $P2_1/a$ coexisted as the minor component in **1c**.

Photoluminescence Φ values were estimated for the crystals of complexes **1a–c** at room temperature in air with an integration sphere (Table 3). The complexes exhibited Φ values of 0.05–0.18

in the crystal. Photostability of the materials is also important in terms of practical application. When the materials were irradiated with UV light at 310 nm (6.5 mW cm^{-2}) at room temperature in air, the intensity of luminescence gradually decreased with keeping the spectral shape as shown in Fig. S11 for complex **1c** as a representative example: the intensity of the luminescence decreased by half within one hour. While the Φ values and photostability may be insufficient for commercial applications, the Au complexes prepared in this study show phosphorescence in air at room temperature (~23 °C), which is very favourable for their use as materials in organic light-emitting devices. Photostability of the materials is also important in terms of practical application. At present, we have not evaluated the long-term photostability of the prepared complexes, but when the materials were irradiated with UV light at 310 nm (6.5 mW cm^{-2}) for several hours, no significant change in the intensity and the spectral shape of luminescence was observed.

Table 3. Photophysical parameters of complexes **1** in crystalline phase at 23 °C.

	τ (μs) ^a	Pre-exponential factor (%)	Φ
1a	33 (13)	—	0.18
1b	40 (15)	—	0.05
1c	15 (59)	95	0.11
	41 (82)	5	

^a 95% confidence interval was indicated in the parentheses.

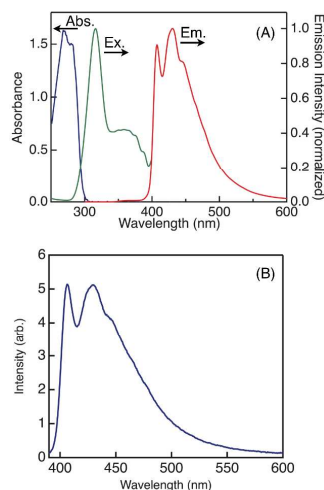


Fig. 6 (A) Absorption, photoluminescence, and excitation spectra of complex **1b**: absorption spectrum in CH_2Cl_2 solution ($1 \times 10^{-4} \text{ mol L}^{-1}$) (blue); photoluminescence in crystalline phase ($\lambda_{\text{ex}} = 310 \text{ nm}$) (red); excitation spectrum in crystal ($\lambda_{\text{em}} = 430 \text{ nm}$) (green). (B) Photoluminescence spectra of **1b** in CH_2Cl_2 solution at concentrations of $1 \times 10^{-4} \text{ mol L}^{-1}$ (blue) and $1 \times 10^{-6} \text{ mol L}^{-1}$ (red).

Photoluminescence spectra of **1a–c** were also measured both in

the Sm phase and isotropic (I) phase. Fig. 7A shows normalised photoluminescence spectra of complex **1b** in the crystalline and SmC phases as a representative example. The complexes showed photoluminescence in the Sm phases, showing a decrease in the absolute intensity of luminescence with thermal phase transition to the Sm phase (Figs. S7–9 for **1a–c**). During this experiment, all experimental conditions, namely all instrumental parameters (band pass of both excitation and emission slits = 5 nm), excitation wavelength (310 nm), power of excitation light (6.5 mW/cm²), were strictly kept constant. Moreover, since the optical densities of the samples used in photoluminescence spectroscopy in the condensed phases were larger than 3, we considered that the samples completely absorbed excitation light in all phases, meaning that the same amount of the excited states was produced in all phases by excitation with the same excitation power.

Therefore, we can compare the intensity of luminescence at least qualitatively in various phases, although the quantum yields were not able to measure in LC and I phases with our instruments. Generally, the intensity of photoluminescence is reduced at a higher temperature because the thermally activated internal molecular motion deactivates the excited states. Thus, it is normal to observe a lower photoluminescence intensity in the Sm phase than in the crystalline phase. An abrupt change in the luminescence intensity was observed in the phase transition to the I phase in all complexes; luminescence was completely quenched in the I phase. Luminescence intensity was recovered when cooling the I phase sample to re-obtain the Sm phase, demonstrating that a reversible “on–off” switching of photoluminescence is possible through inducing phase transition between Sm and I phases. Since each molecule shows vigorous micro-Brownian motion and is oriented randomly in the I phase, the molecular aggregate structures become random with dissociated molecules existing as the isolated monomeric form (Fig. 5); we suggest that it is for this reason that luminescence completely disappeared in the I phase.

As shown in Fig. 7A, the photoluminescence spectral shape and emission maxima of complex **1b** in the crystalline phases (Cr₁ and Cr_x) were the same as those in SmC phase upon heating. However, in the crystalline phase (Cr_x) obtained after recrystallisation from the melt after cooling, the emission maximum was shifted by 35 nm to a longer wavelength, which was accompanied by a change in the spectral shape. When the Cr_x crystal phase was melted again to yield the SmC phase, the emission maximum and spectral shape returned to the initial state. The Commission Internationale de l’Eclairage (CIE) chromaticity diagram allows for quantitative evaluation of photoluminescence colour as shown in Fig. 7B. The luminescence colour was deep blue in the Cr₁ and SmC phases, and was pale bluish-green in the Cr_x phase: the CIE coordinates (x, y) were (0.17, 0.10) in the Cr₁ phase at 40 °C on first heating, (0.18, 0.13) in the SmC phase at 130 °C, and (0.21, 0.29) in the Cr_x phase at 40 °C. These results indicate that the colour of photoluminescence can also be reversibly controlled by phase transition between the Cr_x and SmC phases.

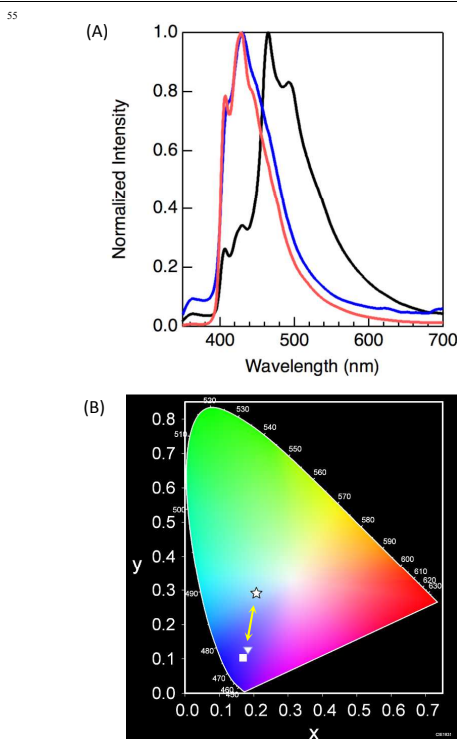


Fig. 7 (a) Normalised photoluminescence spectra of **1b** in various phases ($\lambda_{ex} = 310$ nm): Cr₁ at 40 °C (red); SmC at 130 °C (blue); Cr_x at 40 °C (black). (B) CIE chromaticity diagram for the photoluminescence of **1b**: Cr₁ (□); SmC (∇); Cr_x (○).

As previously described (Fig. 4), the XRD pattern of the Cr₁ phase of **1b** was obtained by simulation from single-crystal X-ray analysis, which revealed that the molecules were packed in the lattice with tilting similar to the SmC phase (Fig. 5). Thus, it is reasonable that a similarity in luminescence spectra, (*i.e.*, same spectral shape and emission maxima) exists for both Cr₁ and SmC phases (*viz.* Fig. 7A). However, in the Cr_x phase, d_{001} -spacing was estimated as 16 Å by XRD (Fig. 4C), which is very similar to the molecular length of the monomer of **1b** (17.9 Å). XRD measurements indicated that the molecules were packed in the lattice without tilting in the Cr_x phase (Fig. 5). These results suggest to us that the aggregated structure is almost the same in the Cr₁ and SmC phases, but is quite different in the Cr_x phase obtained after recrystallisation from the molten states. Thus, this difference in the aggregated structure may result in the change in photoluminescence colour of **1b** induced by the thermal phase transition between Cr_x and SmC phases. Although photoluminescence from complex **1b** should be assigned as a monomer emission, its luminescence is emitted in the aggregate form, the properties of which are dependent on the aggregated structure. At present, the reason for this thermochromic photoluminescence by control of the aggregated structure of **1b** is unclear, owing to a lack of information on the electronic mechanism of luminescence in the present system.

In contrast, the other Au complexes (**1a** and **1c**) did not show changes in colour or spectrum shape of photoluminescence with the phase transition (Figs. S7 and S9). The XRD patterns of **1a** and **1c** are also shown in Figs. S4 and S5; however, the XRD of complex **1a** could not be measured in the LC phase because of insufficient quantity of the sample. The tilted aggregated structures were observed in both Cr₂ and LC phases of complex **1c**; namely, the aggregated structures in both phases were almost the same. Therefore, it is quite reasonable that the complexes show the same colour of luminescence in both phases.

Conclusions

In this study, we synthesised LC complexes containing Au(I) and investigated their phase transition behaviours and photophysical properties. The luminescence intensity of the complexes was enhanced in the condensed phases, a characteristic that is very favourable for the practical application of those complexes in light-emitting devices. Observed photoluminescence behaviour in the condensed phases could be assigned to a monomer emission. In contrast, the luminescent properties were strongly affected by the aggregated structures of the complexes; a reversible “on–off” switching of luminescence was demonstrated by inducing the transition between ordered and disordered aggregates, *i.e.*, the phase transition between the LC and I phases. Moreover, the colour of luminescence could be reversibly controlled *via* the transformation between ordered aggregates; namely, the thermal phase transition between Cr and SmC phases. From the results described above, we can expect Au LC complexes to show great potential in applications involving active colour- and intensity-controllable light-emitting materials.

Experimental

Materials

The Au(I) complexes (**1a–c**) were synthesised from the corresponding isocyanide ligands and (tht)AuCl.⁹ Unless otherwise noted, all solvents and reagents were purchased from commercial suppliers and were used without further purification. ¹H NMR spectra were recorded on a JEOL ECS-400 spectrometer at 400 MHz using the residual proton in the NMR solvent as an internal reference. Electrospray ionisation mass spectra (ESI-MS) were measured on a JMS-T1000LC (JEOL) instrument. MALDI-TOF mass spectra were measured on a Bruker Autoflex II instrument with dithranol (Aldrich) as a matrix. Infrared (IR) spectra were recorded on a JASCO FT/IR-4100 spectrometer using a KBr pellet. Phenyl isocyanide ligands and (tht)AuCl were synthesised according to a literature procedure.^{9,14}

1a (*n* = 5). 4-Pentyloxyphenyl isocyanide (92 mg, 0.49 mmol) and (tht)AuCl (156 mg, 0.49 mmol) were suspended in 9 mL of acetone, and the resulting suspension was stirred for 2 h. The solids in the reaction mixture were filtered off, and the filtrate was evaporated. The obtained white solid was recrystallised from acetonitrile to give the title complex (151 mg, 0.36 mmol) in 74% yield. m.p. 134 °C. ¹H NMR (400 MHz, CD₂Cl₂): δ (ppm) 7.44 (dd, *J* = 7.1, 1.8 Hz, 2H, Ar 2,6-H), 6.94 (dd, *J* = 7.1, 1.8 Hz, 2H, Ar 3,5-H), 3.94 (t, *J* = 6.8 Hz, 2H, OCH₂), 1.80 (quin, *J* = 6.8 Hz, 2H, OCH₂CH₂), 1.37–1.46 (m, 4H, CH₂), 0.93 (t, *J* = 7.0 Hz, 3H, CH₃). FTIR (KBr, cm⁻¹): 3450, 2964, 2934, 2864, 2219, 1598,

1579, 1500, 1392, 1302, 1263, 1242, 1159, 1126, 1072, 1050, 1024, 981, 908. MALDI-TOF-MS (*m/z*): [M + Na]⁺ calcd for C₁₂H₁₅AuCINNaO, 444.04; found, 444.14. Anal calcd for C₁₂H₁₅AuCINO: C, 34.18; H, 3.59; N, 3.32; Au, 46.71. Found, C, 33.82; H, 3.15; N, 3.31; ash, 46.5.

1b–c. According to the above procedure, **1b** and **1c** were obtained from the corresponding phenyl isocyanide in 99% and 63% yields, respectively.

1b (*n* = 6): m.p. 121 °C. ¹H NMR (400 MHz, CD₂Cl₂): δ (ppm) 7.44 (dd, *J* = 7.2, 1.8 Hz, 2H, Ar 2,6-H), 6.94 (dd, *J* = 7.2, 1.8 Hz, 2H, Ar 3,5-H), 3.99 (t, *J* = 6.8 Hz, 2H, OCH₂), 1.80 (quin, *J* = 6.8 Hz, 2H, OCH₂CH₂), 1.31–1.49 (m, 6H, CH₂), 0.91 (t, *J* = 6.8 Hz, 3H, CH₃). FTIR (KBr, cm⁻¹): 3444, 2934, 2860, 2226, 2204, 1600, 1579, 1502, 1468, 1400, 1382, 1304, 1262, 1241, 1160, 1123, 1056, 1020, 988. MALDI-TOF-MS (*m/z*): [M + Na]⁺ calcd for C₁₃H₁₇AuCINNaO, 458.06; found, 458.09. Anal calcd for C₁₃H₁₇AuCINO: C, 35.84; H, 3.93; N, 3.21; Au, 45.2. Found, C, 35.35; H, 3.53; N, 3.17; ash, 42.6.

1c (*n* = 7): m.p. 124 °C. ¹H NMR (400 MHz, CD₂Cl₂): δ (ppm) 7.44 (dd, *J* = 6.9, 2.1 Hz, 2H, Ar 2,6-H), 6.95 (dd, *J* = 6.9, 2.1 Hz, 2H, Ar 3,5-H), 3.99 (t, *J* = 6.8 Hz, 2H, OCH₂), 1.80 (quin, *J* = 6.8 Hz, 2H, CH₂CH₂), 1.31–1.47 (m, 8H, CH₂), 0.89 (t, *J* = 6.9 Hz, 3H, CH₃). FTIR (KBr, cm⁻¹): 3443, 2955, 2927, 2864, 2853, 2220, 1600, 1579, 1502, 1467, 1304, 1261, 1160, 1032, 1009, 998. HRMS-ESI (*m/z*): [M – Cl + CH₃OH]⁺ calcd for C₁₅H₂₃AuNO₂, 446.13943; found, 446.13934. Anal calcd for C₁₄H₁₅AuCINO: C, 37.39; H, 4.26; N, 3.11; Au, 43.80. Found: C, 36.99; H, 3.81; N, 3.10; ash, 44.1.

Phase transition behaviour

LC complex behaviours were observed by POM (Olympus, BX51) equipped with a hot stage (Instec, HCS302 hot-stage and mK1000 controller). The thermodynamic properties of the LCs were determined using DSC (Perkin Elmer, Diamond DSC) at a heating and cooling rate of 2.0 °C/min. At least three scans were performed to check reproducibility. TGA was performed to check the thermal stability of the complexes using a DTG-60AH analyser (Shimadzu) at a heating rate of 5 °C/min. For the sample showing Sm phase, the phase structure was further confirmed and interlayer spacing was estimated by XRD (Rigaku FR-E/R-axis IV) with Cu *K*α radiation (λ = 1.54184 Å).

X-ray crystallography

Single crystals were obtained by slow evaporation from a CH₂Cl₂/hexane (1:2) solution, mounted on a glass fibre, and reflection data were measured using an ω -scan technique on a Rigaku AFC-5R automated four-circular-axis diffractometer with graphite monochromatised Cu *K*α radiation (λ = 1.54178 Å) or a Rigaku R-Axis RAPID two-circular-axis diffractometer with Mo *K*α radiation (λ = 0.71075 Å). The measurements were carried out at room temperature (296 K). The initial structure in the unit cell was determined by a direct method using SIR92.¹⁵ The structure model was refined by full-matrix least-squares methods using SHELXL97.¹⁶ All calculations were performed using the crystallographic software package WinGX.¹⁷ The obtained crystallographic data are summarised in Table S1.[†] When alkyl chains were disordered, the occupancy of atoms was separated

into two parts. The data in Table S1 have been indexed and are included in the Cambridge Crystallographic Centre (CCDC) database with the following reference numbers: CCDC 965148 for **1a**, CCDC 965149 for **1b**, and CCDC 965150 for **1c**. The indexed database contains additional supplementary crystallographic data for this paper and may be accessed without charge at <http://www.ccdc.cam.ac.uk/conts/retrieving.html>. The CCDC may be contacted by mail at 12 Union Road, Cambridge CB2 1EZ, U.K., by fax at (44)1223-336-033, or by e-mail at deposit@ccdc.cam.ac.uk.

Photophysical properties

UV-visible absorption and steady-state photoluminescence spectra were recorded on a JASCO V-550 absorption spectrophotometer and on a Hitachi F-7500 fluorescence spectrophotometer, respectively. For measurements in the crystalline and LC states, the same crystals prepared for the single-crystal X-ray structure analysis were used. The crystals were placed between a pair of quartz plates, and the resultant samples were set on a homemade heating stage to record the spectra at a controlled temperature. Photoluminescent quantum yields were determined using a calibrated integrating sphere system (Hitachi). Photoluminescence decay profiles were measured using a N₂ laser (USHO pulsed dye laser, KEC-160; wavelength 337 nm; pulse width 600 ps; 10 Hz). The emission profiles were recorded with a streak camera (Hamamatsu, C4334; starting delay 55 μ s; integration window 497 μ s).

Supporting Information (See also the footnote on the first page of this article): Full details of synthesis, characterisation of all the complexes, crystallographic data in CIF format, XRD data of crystalline and Sm phases, DSC and TGA thermograms, and details of photophysical characterisations including photoluminescence spectra of all complexes.

Acknowledgment

This work was partly supported by the MEXT-Supported Program for the Strategic Research Foundation at Private Universities, 2012–2016, JSPS KAKENHI (Grant No. 24550217), and JST A-STEP (AS231Z04286D). This research was also supported by the Kyoto Advanced Nanotechnology Network (Nara Institute of Science and Technology), and by the Cooperative Research Program of Network Joint Research Centre for Materials and Devices (Tokyo Institute of Technology).

Notes and references

^aDepartment of Applied Chemistry, College of Life Sciences, Ritsumeikan University, 1-1-1 Nojihigashi, Kusatsu 525-8577, Japan. Fax: +81-77-561-2659; Tel.: +81-77-561-5966; E-mail: tsutsumi@sk.ritsumai.ac.jp

^bPresent address: Department of Organic Chemistry, University of Geneva

† Electronic Supplementary Information (ESI) available: See DOI: 10.1039/b000000x/

1. J. Shinar and V. Savvateev, in *Organic Light-emitting Devices: A Survey*, ed. J. Shinar, Springer, New York, 2004, ch. 1, pp. 1–41.

- (a) Y. Hong, J. W. Y. Lam and B. Z. Tang, *Chem. Commun.*, 2009, 4332; (b) Z. Zhao, J. W. Y. Lam and B. Z. Tang, *Curr. Org. Chem.*, 2010, **14**, 2109; (c) M. Wang, G. Zhang, D. Zhang, D. Zhu and B. Z. Tang, *J. Mater. Chem.*, 2010, **20**, 1858; (d) Y. Hong, J. W. Y. Lam and B. Z. Tang, *Chem. Soc. Rev.*, 2011, **40**, 5361; (e) Z. Zhao, J. W. Y. Lam and B. Z. Tang, *J. Mater. Chem.*, 2012, **22**, 23726.
- (a) J. M. López-de-Luzuriaga, in *Modern Supramolecular Gold Chemistry*, ed. A. Laguna, Wiley-VCH Verlag GmbH & Co. KGaA, 2009, ch. 6, pp. 347–401; (b) R. Gavara, J. Llorca, J. C. Lima and L. Rodríguez, *Chem. Commun.*, 2013, **49**, 72. (c) M. Baron, C. Tubaro, A. Biffis, M. Basato, C. Graiff, A. Poater, L. Cavallo, N. Armaroli, G. Accorsi, *Inorg. Chem.*, 2012, **51**, 1778. (d) M. A. Rawashdeh-Omary, J. M. López-de-Luzuriaga, M. D. Rashdan, O. Elbjairami, M. Monge, M. Rodríguez-Castillo, A. Laguna, *J. Am. Chem. Soc.*, 2009, **131**, 3824.
- (a) J. C. Vickery, M. M. Olmstead, E. Y. Fung and A. L. Balch, *Angew. Chem. Int. Ed.*, 1997, **36**, 1179; (b) A. Kishimura, T. Yamashita and T. Aida, *J. Am. Chem. Soc.*, 2005, **127**, 179; (c) R. L. White-Morris, M. M. Olmstead, S. Attar and A. L. Balch, *Inorg. Chem.*, 2005, **44**, 5021; (d) H. O. Lintang, K. Kinbara, K. Tanaka, T. Yamashita and T. Aida, *Angew. Chem. Int. Ed.*, 2010, **49**, 4241; (e) M. Saitoh, A. L. Balch, J. Yuasa and T. Kawai, *Inorg. Chem.*, 2010, **49**, 7129; (f) S. Han, Y. Y. Yoon, O.-S. Jung and Y.-A. Lee, *Chem. Commun.*, 2011, **47**, 10689; (g) M. Saitoh, A. L. Balch, J. Yuasa, K. Tada, M. Onoda, T. Nakashima and T. Kawai, *Langmuir*, 2011, **27**, 10947; (h) S. H. Lim, J. C. Schmitt, J. Shearer, J. Jia, M. M. Olmstead, J. C. Fettinger and A. L. Balch, *Inorg. Chem.*, 2013, **52**, 823; (i) Y.-P. Zhou, E.-B. Liu, J. Wang and H.-Y. Chao, *Inorg. Chem.*, 2013, **52**, 8629.
- (a) H. Ito, T. Saito, N. Oshima, N. Kitamura, S. Ishizaka, Y. Hinatsu, M. Wakeshima, M. Kato, K. Tsuge and M. Sawamura, *J. Am. Chem. Soc.*, 2008, **130**, 10044; (b) R. L. White-Morris, M. M. Olmstead and A. L. Balch, *J. Am. Chem. Soc.*, 2003, **125**, 1033; (c) S. H. Lim, M. M. Olmstead and A. L. Balch, *J. Am. Chem. Soc.*, 2011, **133**, 10229; (d) C. H. Woodall, C. M. Beavers, J. Christensen, L. E. Hatcher, M. Intissar, A. Parlett, S. J. Teat, C. Reber and P. R. Raithby, *Angew. Chem. Int. Ed.*, 2013, **52**, 9691.
- (a) X. He, W. H. Lam, N. Zhu and V. W. W. Yam, *Chem. Eur. J.*, 2009, **15**, 8842; (b) C. Cordovilla, S. Coco, P. Espinet and B. Donnio, *J. Am. Chem. Soc.*, 2010, **132**, 1424; (c) R. Bayón, S. Coco and P. Espinet, *Chem. Eur. J.*, 2005, **11**, 1079; (d) J. Arias, M. Bardají and P. Espinet, *Inorg. Chem.*, 2008, **47**, 3559; (e) S. Coco, C. Cordovilla, C. Domínguez and P. Espinet, *Dalton Trans.*, 2008, 6894; (f) M. J. Mayoral, P. Ovejero, J. A. Campo, J. V. Heras, E. Pinilla, M. R. Torres, C. Lodeiro and M. Cano, *Dalton Trans.*, 2008, 6912.
- (a) I.-C. Khoo, *Liquid Crystals*, Wiley Interscience, Hoboken, 2nd edn., 2007; (b) J. L. Serrano and T. Sierra, in *Metallomesogens: Synthesis, Properties, and Applications*, Wiley-VCH Verlag GmbH & Co. KGaA, 2007, ch. 3, pp. 43–129.
- (a) K. Fujisawa, N. Kawakami, Y. Onishi, Y. Izumi, S. Tamai, N. Sugimoto and O. Tsutsumi, *J. Mater. Chem. C*, 2013, **1**, 5359; (b) K. Fujisawa, Y. Izumi, A. Nagamatsu, K. Uno and O. Tsutsumi, *Mol. Cryst. Liq. Cryst.*, 2012, **563**, 50.
- S. Coco, P. Espinet, S. Falagan and J. M. Martín-Alvarez, *New J. Chem.*, 1995, **19**, 959.
- H. Schmidbaur, *Gold Bull.*, 2000, **33**, 3.

-
11. (a) R. E. Bachman, M. S. Fioritto, S. K. Fetcs and T. M. Cocker, *J. Am. Chem. Soc.*, 2001, **123**, 5376; (b) H. Schmidbaur and A. Schier, *Chem. Soc. Rev.*, 2008, **37**, 1931.
 12. E. R. T. Tiekink and J. Zukerman-Schpector, *CrystEngComm*, 2009,
5 **11**, 1176.
 13. (a) E. R. T. Tiekink, J.-G. Kang, *Coord. Chem. Rev.*, 2009, **253**, 1627.
(b) I. O. Koshevoy, E. S. Smirnova, M. Haukka, A. Laguna, J. C. Chueca, T. A. Pakkanen, S. P. Tunik, I. Ospino and O. Crespo, *Dalton Trans.*, 2011, **40**, 7412.
 - 10 14. M. J. Howard, F. R. Heitzler and S. I. G. Dias, *J. Org. Chem.*, 2008, **73**, 2548.
 15. A. Altomare, G. Cascarano, C. Giacovazzo and A. Guagliardi, *J. Appl. Crystallogr.*, 1993, **26**, 343.
 16. G. M. Sheldrick, *Acta Crystallogr., Sect. A: Found. Crystallogr.*, 2008,
15 **64**, 112.
 17. L. J. Farrugia, *J. Appl. Crystallogr.*, 1999, **32**, 837.